*European Journal of Neuroscience, Vol. 12, pp. 1466–1478, 2000* 

# Functional coupling shows stronger stimulus dependency for fast oscillations than for low-frequency components in striate cortex of awake monkey

Axel Frien and Reinhard Eckhorn
Department of Physics, Group of Neurophysics, Philipps University, Renthof 7, D-35032 Marburg, Germany

*Keywords*: gamma-oscillations, object-coding, signal coherence, texture surface

## Abstract

It has been argued that coupling among the neural signals activated by a visual object supports binding of local features into a coherent object perception. During visual stimulation by a grating texture we studied functional coupling by calculating spectral coherence among pairs of signals recorded in the striate cortex of awake monkeys. Multiple unit activity (MUA) and local field potentials (LFP, 1–140 Hz) were extracted from seven parallel broad band recordings. Spectral coherence was dominated by high-frequency oscillations in the range 35–50 Hz and often by additional low-frequency components (0–12 Hz). Functional coupling among separate cortical sites was more stimulus specific for MUA than for LFP: MUA coherence at high and low frequencies depended highly significantly on: (i) the similarity of the preferred orientations at the two sites – the more similar the higher the coherence; (ii) the orientation of the stimulus grating – with highest coherence at half angle between the preferred orientations at the two sites; (iii) cortical distance – coherence decreases to noise levels at ~ 3 mm (MUA) and 6 mm (LFP). Coherence of fast oscillations did not depend on the degree of coaxiality of the orientation-sensitive receptive fields, whereas low frequencies showed significant dependency. This indicates that different frequency components can engage different coupling networks in the striate cortex which probably support different coding tasks. Changes in average oscillation frequency with stimulus orientation were highly significant for fast oscillations while there was no dependency for low frequencies. Finally, stimulus-related spectral power and coherence of fast oscillations were considerably higher than of low frequency components. Fast oscillations may therefore contribute more to feature binding and coding of object continuity than low-frequency components, at least for texture surfaces as analysed here.

## Introduction

### *Coding of object continuity*

Principles of object coding at the lower cortical levels of visual processing are still controversially discussed, including the ongoing debate about feature binding. The latter topic has extensively been investigated in the visual modality by asking how the continuity of visual objects may be coded by visual cortical neurons and how objects are separated from ground. One hypothesis states that this is accomplished by synchronization and desynchronization at a fast time scale, in particular by fast cortical oscillations (e.g. Eckhorn *et al*., 1988; Gray *et al*., 1989; Kreiter & Singer, 1996; Eckhorn, 1999). Other proposals for the temporal coding of scene segmentation rely on relative timing in stimulus-locked transients, in which cortical responses at similar delays are assumed to support binding (e.g. Eckhorn *et al*., 1990; Gawn *et al*., 1996; Opara & Woergoetter, 1996). A recent proposal is based on the simultaneous evaluation of phase relations across multiple recordings in monkey V1 and states that phase continuity may code object continuity (Eckhorn & Gabriel, 1999). It is not clear to date, whether these candidate codes are operational and influence visual scene segmentation. It is beyond the scope of the present work to clarify this, because it requires monkey experiments with reported perceptions. However, evaluations of spatio-temporal relations of different response components and their dependence on stimulation may provide hints as to which components in what visual situations may supply information with respect to scene segmentation. For this, low-frequency components have to be included in calculations of signal coupling in addition to the already existing work in the high-frequency range, because the stimulus-locked components, potentially contributing to scene segmentation, have the highest amplitudes in the 5–10 Hz range. Inclusion of low-frequency correlations in studies of object integration has not been performed yet as far as we know.

Another hypothesis of object-specific coding is based on a spike rate increase in the range of object and a decrease of ground representations. Slightly enhanced spike rates have been reported with textured stimuli at sites of object representations relative to those stimulated with equally textured background in monkey V1 (Lamme, 1995; Zipser & Lamme, 1996). The excess spikes occurred relatively late after stimulus onset (150–250 ms) which was interpreted as an action of 'filling-in' from the object's contour representation, because the latter has a much stronger activation and precedes the activity increase at the object's surface (Lamme *et al*., 1999). These differential spike rates in favour of object surfaces were obtained when object and background were composed of the same texture elements. However, such differences are not sufficient for coding the continuity of an object or separate it from ground because spike rates vary in the striate cortex with local feature contrasts, they generally

*Correspondence*: Dr R. Eckhorn, as above.
E-mail: reinhard.eckhorn@physik.uni-marburg.de

*Received 4 February 1999, revised 14 December 1999, accepted 17 January 2000*

increase with increasing contrast (for luminance contrast see e.g. Sclar *et al*., 1990; Edwards *et al*., 1995; review in Orban, 1984; however, Gawn *et al*., 1996 found spike rates in V1 complex cells independent of luminance contrast). Spike rates may be high in some positions of background and low at parts of a currently interesting object or vice versa, and thus, spike rates per se do not provide unambiguous object coding. On the other hand, stimulus-related changes in activity and their correlative relations do not depend on absolute amplitudes and might therefore better be suited for coding feature relations of a visual object. In addition, it is an open question whether such coding may be accomplished by slow coherent changes in spike rates at the 50–100 ms scale or by fast synchronization and desynchronization at the 5–10 ms scale. Also, other scales and varying mixtures are possible. In any case, different scene segments can evoke different modulations in neural activities specifically depending on the type and timing of visual stimulation. Such stimulus-depending modulations can be detected and quantified by signal correlation methods, including cross-correlation and spectral coherence in parallel recordings. This path is followed in the present investigation.

### *Object contour coding*

Potential coding of object boundaries by coherent signals has extensively been investigated in the visual cortex in states of fast synchronized oscillations. With elongated stimuli (mostly light bars) spike patterns in the striate cortex became rhythmic (35–80 Hz) and strongly synchronized if their receptive fields were coaxially aligned (Eckhorn *et al*., 1988; Gray *et al*., 1989, 1992; Engel *et al*., 1990, 1991a,b; Kreiter & Singer, 1992; Koenig *et al*., 1995a; Munk *et al*., 1996; for a review see Kreiter & Singer, 1996). This finding together with related modelling work (e.g. Eckhorn *et al*., 1990) suggested that recurrent lateral connections facilitate and synchronize neurons representing elongated contours. Other work on contour coding concentrated on changes in spike rates (Ts'o *et al*., 1986; Gilbert *et al*., 1996). They found weak but significant spike rate modulations in orientation-sensitive V1 neurons with coaxially aligned receptive fields which was understood as an action of common inputs or mutual facilitation supporting the coding of elongated contours.

Several psychophysical studies also showed facilitatory interactions along object contours by demonstrating increased sensitivity at coaxially aligned positions to orientated small patches of Gabor gratings (e.g. Field *et al*., 1993; Kapadia *et al*., 1995; Polat *et al*., 1998; Ito *et al*., 1998). Further support to facilitation along contours was given by measurements of visual evoked potentials (VEPs) in humans showing that collinear stimuli induced VEP facilitation while non-collinear stimulus combinations did not (Polat & Norcia, 1996). In summary, these data suggest that in the visual cortex lateral coupling circuits support feature binding at elongated object contours by orientation-sensitive neurons with coaxially aligned receptive fields. However, recent psychophysical work disputed the necessity of coaxial alignment of local texture elements to a contour for its easiest detection (Keeble & Hess, 1998). Instead, coaxially aligned Gabor patches of equal orientation were reported to have the same thresholds as those of different orientations or if Gaussian or bulls-eye blobs were used. Hence, facilitation at collinear positions is supported by the results of Keeble and Hess, but this effect was largely independent of the orientation of the local stimulus features in their work.

### *Object surface coding*

Despite contour coding, a second equally important aspect in object coding is the representation of its surface. For this task, generally local features of similar properties (e.g. similar colour, orientation, texture) have to be integrated equally well in any spatial direction across the surface (Wertheimer, 1923). Thus, if surface coding is supported by coupled lateral cortical networks these should have different connectivities compared with that for contour coding.

A specific role of correlated slow signal modulations for surface coding (including spike rates) has not been investigated yet as far as we know. Only indirect information is available about object-specific rate modulations (Lamme, 1995; Zipser & Lamme, 1996). This is in part the aim of the present work in which we compare signal coherence in the high-frequency range (31.3–62.5 Hz) with coherence at lower frequencies.

For this, we recorded broad band signals from the striate cortex of awake monkeys while the neurons were activated by large grating textures representing surface features without disturbance from object boundaries. Extraction of different signal components and calculation of their mutual spectral coherence then enabled us to test the components in their potential contribution to surface coding. If coding of surface continuity is significantly influenced by signal coupling among cortical neurons, we expect the highest coherence among neighbouring neurons coding similar features (e.g. similar orientation preference). But unlike for contour coding with the strongest coupling among coaxially aligned receptive fields, coherence should be independent of the relative directions, including oblique and parallel receptive field positions. The results of our present paper support this expectation. (Preliminary results have been reported as a conference report, Frien *et al*., 1996.) An accompanying paper shows that fast oscillations display sharper orientation tuning than signals at lower frequencies, including spike rates (Frien *et al*., 2000).

## Materials and methods

We quantified neural coupling by calculating spectral coherence among recording sites with any orientation preference at a range of several millimetres cortical separation. As considerable spectral power was present in the low- and high-frequency ranges, but often minor power in the medium range of the broad band recording, we restricted the coherence analysis to the frequency bands containing relevant power (low : 0–11.7 Hz; high : 31.3–62.5 Hz).

### *Experiments*

Experiments were performed on two awake macaque monkeys (for details, see Eckhorn *et al*., 1993; Frien *et al*., 2000). From the raw broad band recordings (1 Hz to 10 kHz; both 12 db/octave) we extracted multiple unit activity (MUA: raw signals bandpassed at 1–10 kHz; full wave rectified; low passed at 140 Hz) and local field potentials (LFP: raw signal filtered between 1 and 140 Hz; 12/30 dB/oct) from each of up to seven μ-electrodes. Signal prefilterings were performed by hardware precision Bessel filters (amplitude and phase errors < 2%). Classical receptive fields were characterized according to their position, size and orientation preference on the basis of MUA peri-stimulus time histograms. The corresponding receptive fields were stimulated by a spatial grating (sinusoidal intensity modulation at near optimal spatial frequency) drifting behind an aperture of 20° diameter across the receptive fields while the monkey maintained fixation. In each trial the direction of movement was randomly chosen from a set of eight equally separated directions (for more details see accompanying paper, Frien *et al*., 2000). All procedures were approved by an official German animal care and use committee, and followed the NIH Principles of Laboratory Animal Care (Publication 86–23, revised 1985).

### Data analysis

#### Coherence

For all combinations of recording pairs of the seven-electrode array we determined the spectral coherence (Glaser & Ruchkin, 1976; Bullock & McClune, 1989) for the respective MUA and LFP signals on the basis of sliding windows (width: 128 bin = 256 ms; shifting interval: 64 bin = 128 ms). The coherence function was used to quantify the frequency-dependent correlation between pairs of electrodes [Eq. (1)]:

$$\gamma^2(f) = |C_{xy}(f)|^2/[C_{xx}(f) \cdot C_{yy}(f)] \quad (1)$$

$C_{xy}(f)$ denotes the complex cross-spectrum of signals $x$ and $y$ averaged over trials with identical stimulation, $C_{xx}(f)$ and $C_{yy}(f)$ are the power (auto-) spectra of signals $x$ and $y$. The coherence function is normalized to the range [0, 1], it reveals the constancy of relative phase over trials and the degree of amplitude covariation. The coherence of different recordings was first Fisher-$z$ transformed and then averaged according to the respective directions of stimulus movement. The resulting values were transformed back by the inverse Fisher $z$-transformation. For further analysis we averaged the responses for opposite movement directions as we found no significant difference between them (opposite movement directions had the same orientation of the grating's stripes).

The coherence values of single windows were separately averaged for trials recorded during identical stimulation ($n = 16$ for each recording position): averaging was performed along trials (temporal average), and across trials (ensemble average) which led to window counts of ~300 for each stimulus orientation at each recording position. Therefore, correction for bias due to low sample numbers was not necessary (Glaser & Ruchkin, 1976).

#### Normalizations

To obtain meaningful average results of signal coupling among the broad diversity of preferred orientations in V1 neurons we performed a normalization with respect to rotation and translation. For rotational normalization the absolute orientation preferences of pair recording sites were changed to a common zero orientation (Fig. 1). This was made by calculating the direction of the vector at half the angle between the two preferred orientations and rotating it to zero (3 o'clock) together with the orientation tuning curves. The translational normalization was performed by shifting one of the two receptive fields into the origin (of a Cartesian coordinate system) while leaving the RF-separations and their relative orientations unchanged (Fig. 1B). With both normalizations together we can represent average cortical coupling properties among a centre reference position and other positions at any cortical distance. We transformed these cortical coupling fields to visual space according to the receptive field distances of the recording pairs and call it visual 'coupling field' or visual 'association field' (Eckhorn *et al*., 1990). In the present investigation the coupling strengths in the association fields are quantified by the coherence which is coded for each recording pair by a grey level (the higher the coherence the darker the dot; Fig. 1B, and Figs 4 and 5).

Coaxiality is an angle of orientation classified according to the relative arrangement of the receptive fields and their preferred orientations. The imagined line between two receptive field centres serves as line of reference. The highest coaxiality among two recording positions is present if the preferred orientations are identical to that of the reference line. The lowest coaxiality is present with two orientation preferences orthogonal to the reference line (this is a case of highest co-orientation). Intermediate values are calculated from the average deviation angle of the two orientation preferences relative to the reference. In analogy to the angle between preferred orientations we created three classes of coaxiality (0–30°, 30–60°, 60–90°) to distinguish between different degrees of coaxiality.

#### Orientation index

For comparison of the low- and high-frequency ranges we evaluated various dependencies. For the effect of stimulus orientation on coherence, an orientation index (OI) was calculated.

$$OI = \frac{(P(0^\circ) - P(90^\circ))}{\sum_i P(i)}; \qquad i \in \{0^\circ, 45^\circ, 90^\circ, 135^\circ\} \quad (2)$$

$P(i)$ is the response to the $i$-th stimulus orientation. Usually $P(0°)$ had the highest response value and $P(90°)$ the lowest which results from the above-mentioned rotation of the preferred orientation to 0°. For the difference between preferred orientations, an index PI was defined in a similar way as OI.

To quantify the distance dependence of coherence we estimated the spatial decay constant $d_0$:

$$c = c_r + c_0 e^{-d/d_0} \qquad c_r \sim 0 \quad (3)$$

$$d = d_0 \ln(c_0) - d_0 \ln(c) \quad (4)$$

Detailed analysis of parts of the presented data had shown that the decay of coherence $c$ with cortical distance could be approximated by an exponential function like Eq. (3) with a vanishing residual coherence $c_r$ for large distances (Frien *et al*., 1996). The natural logarithm leads to Eq. (4), and a linear regression gives an estimate for the decay constant $d_0$.

#### Statistical test of significance

The averaged results were sorted into three classes according to the differences between preferred orientations at pair recording sites (0–30°, 30–60°, 60–90°), and into six classes according to their cortical distance as given by the interelectrode spacing (750 µm). Each of these classes may have contributions from a variety of different recording pairs. The mean values of coherence and peak frequencies in the low-frequency (0–11.7 Hz) and high-frequency range (31.3–62.5 Hz) were statistically tested for dependence on cortical distance, on the orientation of the stimulus, on the angle between preferred orientations, and on the degree of coaxiality by a multivariate analysis of variance.

## Results

In 19 sessions (monkey A: 10; monkey B: 9), we recorded MUA and LFP from up to seven electrodes in parallel. In total we obtained data from 202 striate cortex sites (A: 119; B: 83). For further analysis we excluded only 19 sites (A: 18; B: 1) that were not orientation specific on the basis of averaged MUA responses (see Table 1 for the respective numbers of combinations between these positions in relation to the cortical distance, the degree of coaxiality, and the angle between preferred orientations).

### Coherence

To compare the coherence at different spectral frequencies in pairs of recording positions we searched for the spectral maxima in the ranges 0–11.7 Hz (low) and 31.3–62.5 Hz (for the selection of frequency bands see accompanying paper: Frien *et al*., 2000). These bands turned out to be most strongly activated by the visual stimulation. For

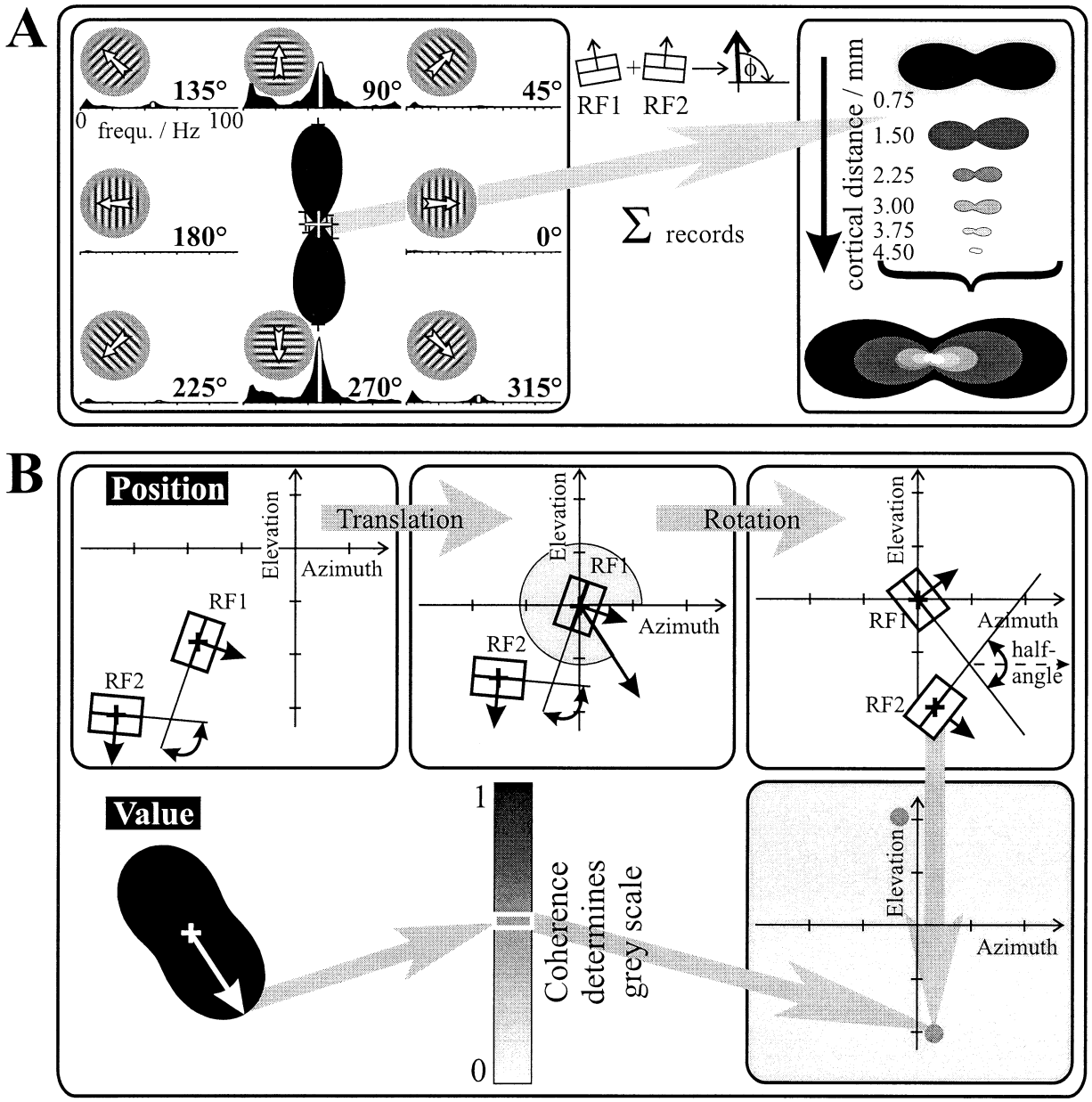


FIG. 1. Evaluation of coupling strength among pairs of cortical recording sites. Schematic construction of normalized polar orientation tuning of peak coherence (A) and 'association fields' (B). (A) Left box: calculation of a polar plot where the amplitude is given by the strength of coupling among two cortical recording sites. Coupling strength is quantified by the spectral coherence, here at the peak in the high-frequency range. These values are indicated by the white bars in the coherence spectra, surrounding the polar plot. They are shown for each of the eight stimulus movement directions. In this example the coherence is maximal at a stimulus orientation of ~90° (see symbols between left and right box). (A) Right box: normalization of tuning orientation. The coherence tuning curve is rotated with its maximum to zero (i.e. to horizontal). The rotated coherence tuning curves of all recording pairs belonging to the same class were averaged (see Fig. .3) for the following different classes: (i) cortical distance; (ii) difference of preferred orientations; and (iii) degree of coaxiality among pair recording sites. In the right box coherence tunings are shown in a single plot for the six cortical distances of pair recordings (between boxes: example for nearly coaxial receptive fields). (B) Construction of 'association fields', which specify the estimated average distribution of cortical coupling strength projected to the visual field. Consecutive operations are shown in the boxes from upper left to lower right. Left: two positions of simultaneously recorded receptive fields in Cartesian visual space and their preferred movement directions. Middle: the origin of the Cartesian coordinate system is shifted to one of the RFs. Upper right: the pair of RFs is rotated to an orientation given by the vector half between the preferred orientations (this direction is chosen because grating stimuli drifting in this direction produced the largest coherence). Rotation is to azimuth (zero) around the RF at the origin. The distance and relative angles among the RFs are preserved by this normalization. The value of peak coherence among a recording pair is encoded as grey value at the normalized position of the receptive field RF2. As RF positions of recording pairs were treated equivalently, each recording pair resulted in two positions symmetrical to the origin.

each cortical distance of the pair recordings we integrated the power over an interval of ± 3 Hz around the respective spectral maximum. Power integration was performed by fitting a Gaussian to the spectral peak and integrating over ± 3 Hz around the peak. This ensures a better separation of the oscillatory components around the peak from the broad band background activity that is often not stimulus depending. From these peak coherence values we calculated direction-tuning curves of coherence. Figure 2 shows this exemplary for one pair of simultaneously recorded multi-unit activities. Original traces of responses to identical stimulus repetitions are shown

TABLE 1. Numbers of paired recordings according to cortical distance, degree of coaxiality and difference in preferred orientation

| Coaxiality/ Δ–orientation | Cortical distance between recording electrodes | | | | | | |
|---|---|---|---|---|---|---|---|
| | 0.75 mm | 1.50 mm | 2.25 mm | 3.00 mm | 3.75 mm | 4.50 mm | Totals |
| 0–30°/ | | | | | | | |
| iso | 13 | 3 | 11 | 5 | 3 | 1 | 36 |
| oblique | 17 | 25 | 8 | 6 | 6 | 1 | 63 |
| ortho | 18 | 10 | 6 | 10 | 5 | 1 | 50 |
| 30–60°/ | | | | | | | |
| iso | 5 | 8 | 10 | 10 | 7 | 1 | 41 |
| oblique | 27 | 19 | 17 | 7 | 3 | 4 | 77 |
| ortho | 15 | 9 | 3 | 11 | 4 | 1 | 43 |
| 60–90°/ | | | | | | | |
| iso | 13 | 9 | 4 | 5 | 7 | 3 | 41 |
| oblique | 7 | 12 | 16 | 7 | 5 | 4 | 51 |
| ortho | 15 | 14 | 8 | 8 | 4 | 5 | 54 |
| Totals | 130 | 109 | 83 | 69 | 44 | 21 | 456 |

Δ-orientation: difference in preferred orientations of neurons at the pair recording sites. Coaxiality: highest coaxiality has pair recording positions whose orientation preferences are identical and has the orientation of the line connecting their receptive field centres (see also Materials and methods).

together with their auto- and cross-spectra for one of eight stimulus movement directions. Analysis of all stimulus directions revealed a remarkable orientational tuning not only for the auto (power) spectra (not shown) but also for the cross-spectra (see Fig. 1A).

The investigated parameters of the present analysis were the cortical distance, the angle between the preferred orientations of the respective receptive fields, the direction of stimulus movement and the degree of coaxiality. To work out different aspects of interdependence between these parameters we combined them in two different ways, as polar directional tuning of coupling strength (coherence) as shown in Fig. 1A, and as visual association fields (see Materials and methods, and Figs 4 and 5).

### High-frequency range

#### *MUA coherence*

We separated pairs of recording positions according to their difference angle between preferred orientations and to their degree of coaxiality. Each of the nine plots in Fig. 3 shows polar orientation tunings of high-frequency MUA coherence for the six analysed cortical distances. It turned out that nearly each of these coherence characteristics is strongly dependent on the orientation of the stimulus grating. Furthermore, there is a consistent tendency for coherence to decrease with cortical distance. The multivariate analysis of variances shows both effects to be strongly significant. Comparison of coherences for the three classes of differences between preferred orientations (columns in Fig. 3) reveals a less pronounced but still highly significant effect ($P < 0.001$). This is higher coherence among recording sites with similar orientation preference and lower coherence among nearly orthogonal sites. The degree of coaxiality (rows in Fig. 3) had no significant effect on the spectral coherence of neural signals in our investigation (for details see Table 2).

#### *LFP coherence*

LFP coherence strongly depends on cortical distance, as does MUA coherence. However, LFP coherence depends only weakly on the difference of preferred orientations and the other parameters have no significant influence at all.

#### *Frequencies of fast oscillations*

Besides the value of coherence, we analysed the dependence of the oscillation frequency at the dominating high-frequency peak on the above-mentioned parameters. We found a highly significant dependence of this frequency on stimulus orientation ($P < 0.001$) for MUA as well as for LFP. None of the other parameters revealed even a slight tendency towards significance (Table 2).

### Low-frequency range

#### *Coherence*

For MUA, the spectral coherence depends significantly on all parameters under investigation ($P < 0.01$), while the LFP coherence depends only on cortical distance and the degree of coaxiality, but this is highly significant ($P < 0.001$). Furthermore, the peak frequencies for MUA as well as for LFP depend significantly on the degree of coaxiality ($P < 0.01$).

### Comparison of high- and low-frequency ranges

#### *Dependences on cortical distance*

All coherence values but none of the peak frequencies depend on cortical distance irrespective of the examined frequency range and irrespective of the type of signal (MUA or LFP). To evaluate distance dependence we estimated the spatial coupling decay by fitting with an exponential function (see Materials and methods). This revealed coupling ranges (space constant $d_0$) being significantly greater for low- than high-frequency components, irrespective of the type of signal (LFP and MUA; $P < 0.001$). For fast oscillations it is significantly greater for LFP compared with MUA ($P < 0.001$). MUA and LFP decay constants for low frequencies show no significant differences. (The significance criteria are corrected according to Bonferroni's theorem).

#### *Dependence on coaxiality*

While in the low-frequency range all the MUA and LFP coherences as well as the dominant frequencies turned out to depend significantly on the degree of coaxiality, none of the high frequency *P*-values reached the level of significance.

#### *Dependence on difference in preferred orientations*

The MUA coherences in the low- as well as high-frequency range depend highly significantly on the difference of the preferred orientations. Quantification of this dependence by the index PI (see Materials and methods) reveals no significant difference between the frequency ranges (paired *t*-test).

*Dependence on stimulus orientation*

The MUA coherence of low and high frequencies and the peak frequencies of MUA and LFP in the high-frequency range depend on stimulus orientation. We compared the strength of these dependencies by calculation of an orientation index (OI; see Materials and methods). The OI of the fast oscillations' coherence turned out to be greater than that of the low frequencies ($P < 0.001$; paired $t$-test). Thus, the dependence on stimulus orientation is significantly stronger in the high- than low-frequency range.

### *Association fields*

Besides these statistically testable general effects, we visualize average coherence values for specific combinations of parameters in association fields (see Materials and methods, and Eckhorn *et al*., 1990). Although this concept already presents the results of average spatial coupling in a highly condensed form, it is not useful to show all association fields for MUA and LFP, for low- and high-frequency ranges, for all differences between preferred orientations and for all the eight directions of stimulus movement. Because of the qualitatively high similarity between the association fields for the different directions of stimulus movement, only the data for zero degree orientation are shown for MUA (Fig. 4) and LFP (Fig. 5).

The association fields from multi-unit activity (Fig. 4) show the strong decline of coherence with distance for the low- and high-frequency ranges. Despite this general dependence we found lower average values of coherence for short cortical distances up to 0.5 mm compared with the coherence for distances from 0.5 to 1.0 mm. This effect is highly significant for the fast MUA oscillations tested over all directions of stimulus movement and over all three classes of differences of preferred orientations ($t$-test; $P < 0.001$). Local field potentials and low-frequency MUA were tested in the same way, but the coherence for these two distance ranges are not significantly different. For Fig. 6 the cortical recording distances are transformed to visual space, representing the dependence of coherence on the separation of receptive field centres. Coherence of fast MUA oscillations turned out to be maximal for separations of ~0.33° visual angle (Fig. 6, upper right) while there is a monotonous spatial decline for low-frequency MUA coherence as well as for LFP coherence in both frequency ranges.

## Discussion

### *Major results*

We are interested in the functional coupling among distributed sites of the striate cortex in order to understand principles of object coding at low levels of visual cortical representations. As coupling among high-frequency oscillatory components has previously been suggested to support feature integration (e.g. Eckhorn *et al*., 1988; Gray *et al*., 1989), and other work proposed transient stimulus-locked lower frequency components to support object binding (e.g. Eckhorn *et al*., 1990; Gawn *et al*., 1996; Opara & Woergoetter, 1996), we quantified functional coupling by calculating spectral coherence at low and high frequencies from the same broad band recordings during stimulation by a texture surface. Two results seem especially important.

**1** High-frequency power and cortical coupling (measured by coherence) generally depend more strongly on stimulation parameters than power and coupling at low frequencies. In particular, high-frequency coherence strongly depends on the relative orientation preferences at the pair recording sites. Coherence is higher the more similar the orientation preference, the better the neurons are driven by the grating and the nearer they are in cortical and visual space, resembling Gestalt rules of proximity and similarity (Wertheimer, 1923; Kramer & Jacobson, 1991; Polat & Norcia, 1996). This suggests a more important role of high compared with low frequencies for coding orientated texture surfaces in V1.

**2** Coupling strength at high frequencies is uniformly distributed in cortical, and hence in visual space. This suggests that high-frequency coupling can flexibly match to spatial aspects of stimulus context. In the present investigation, the cortical network engaged in a homogeneous coupling across the representation of similar features,

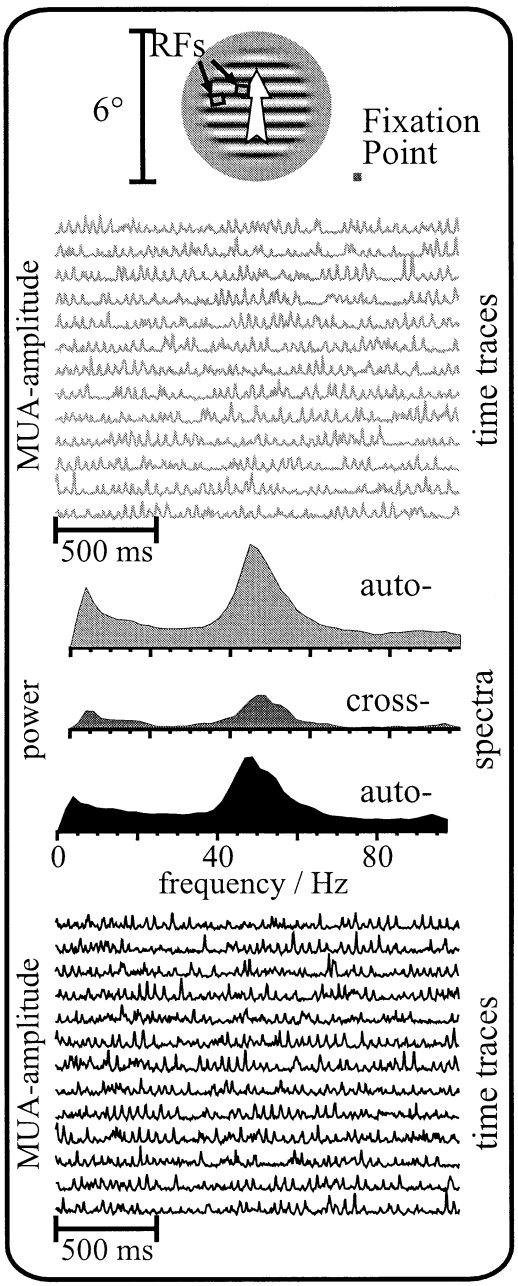


FIG. 2. Original response traces and corresponding auto- and cross-spectra of fast oscillations in multiple unit activity (MUA). Example of 13 consecutive response epochs to identical stimulation from two simultaneously recorded sites for the optimal direction of stimulus movement. Auto- and cross-spectra are averages obtained for ~3-s epochs. The arrangement of visual stimulus and receptive fields relative to the point of fixation is shown on the top. Note the dominance of fast oscillations over the remaining part of the spectrum. (For examples of original MUA and LFP responses with the same stimulus see fig. 2 of the accompanying paper, Frien *et al*., 2000).

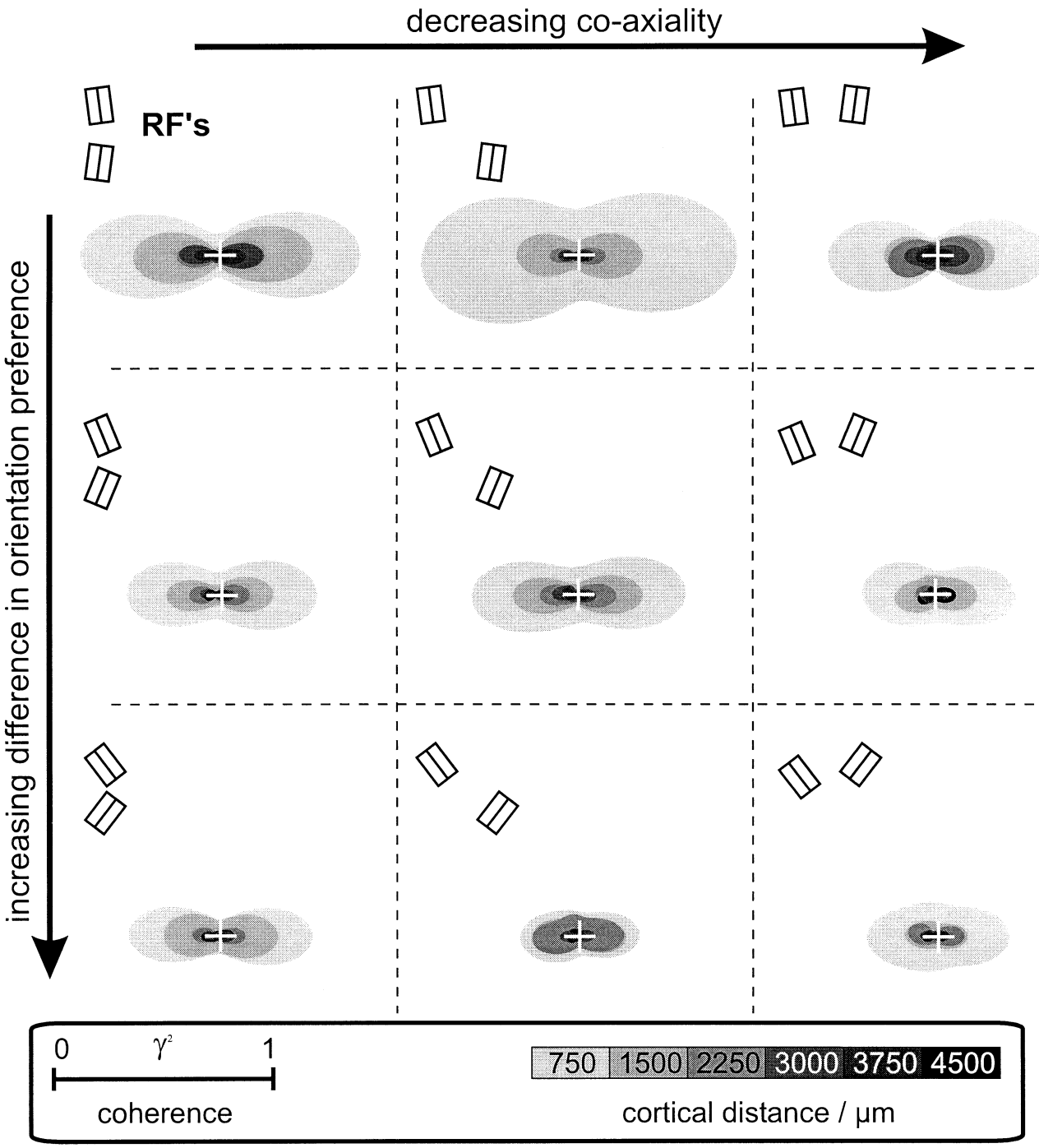


FIG. 3. Coupling among fast oscillations at separate cortical sites depends on stimulus orientation, on the coaxiality, and on the difference in preferred orientations of the receptive fields at the two sites. Multiple unit activity (MUA) recorded simultaneously in V1. Polar tunings of dominant components for three classes of receptive field coaxiality (columns) and three classes of difference in preferred orientation (rows). Cortical distance is encoded by grey value (scale bar at lower right). Coupling strength is measured by the coherence values that are given by the radius (scale at lower left). Averages are calculated from responses to 16 identical stimulus repetitions for each grating orientation and recording position. For further details see Materials and methods.

FIG. 4. 'Association field' determined from multiple unit activity (MUA). Distribution of average cortical coupling strength among pair recording positions projected to the visual field. Coupling strength is quantified by the spectral coherence in two frequency bands (low: 0–11.7 Hz; and high: 31.3–62.5 Hz). Positions in the visual field are normalized to the receptive field centres at one site of the pair recording (cross bar at centre), while the dot position indicates the distance and direction of the RF-centre at the second site (position of grey spot in the plot). In other words: the spot's position relative to the centre cross indicates the distance and relative positions of the RFs of a cortical recording pair, it does not indicate the absolute positions of RFs relative to the fixation point. Coherence is indicated by the grey level of the spots (lower right), plotted for the three classes of differences in preferred orientations at pair recording sites (first row: 0–30°, 'similar'/second row: 30–60°, 'oblique'/third row: 60–90°, 'orthogonal'/mean eccentricity relative to the foveal centre was 2.5–4.5° visual angle. The direction of stimulus movement: 0°, i.e. to the right).

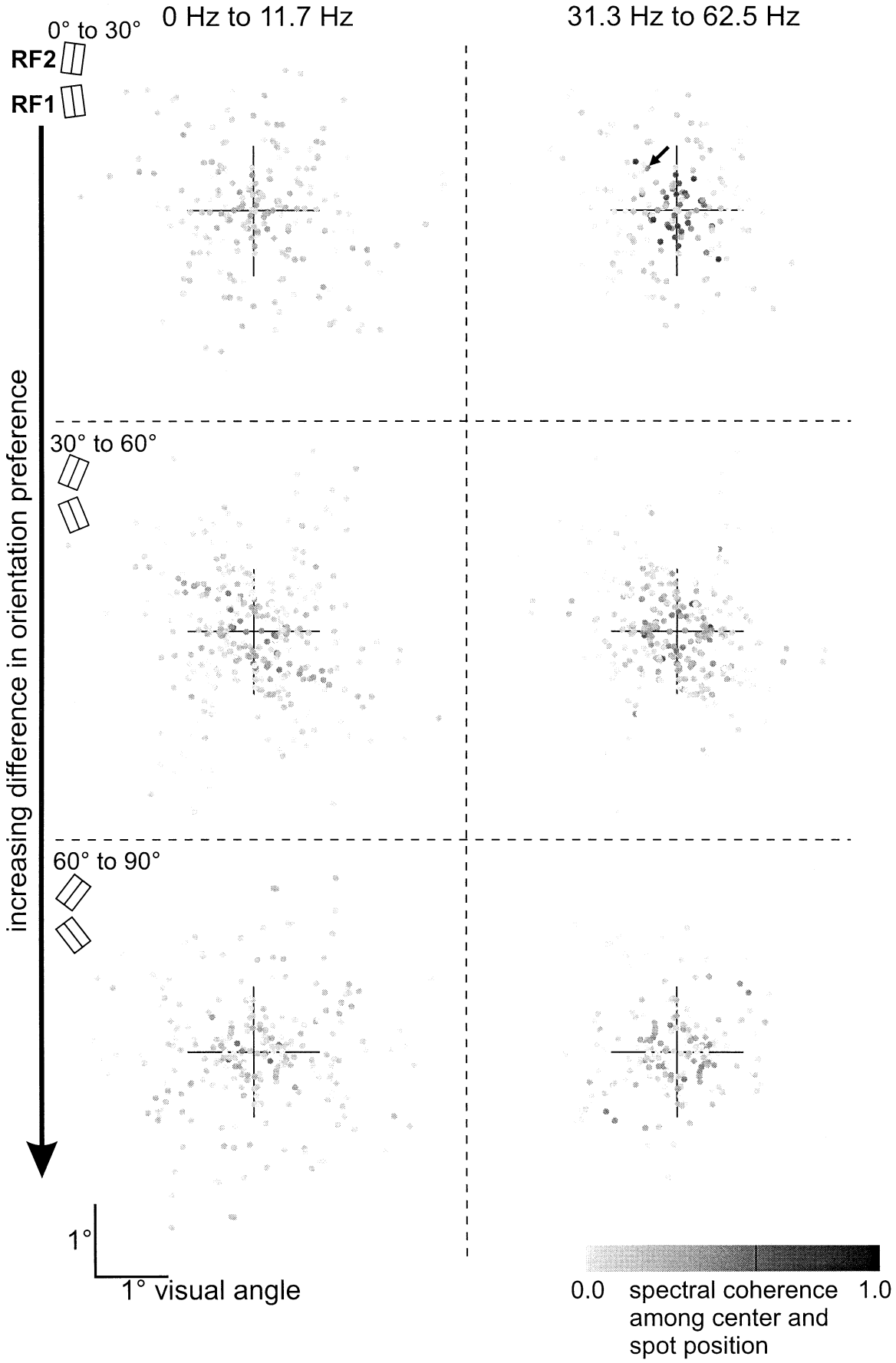
0 Hz to 11.7 Hz
31.3 Hz to 62.5 Hz
0° to 30°
RF2
RF1
30° to 60°
60° to 90°
increasing difference in orientation preference
1°
1° visual angle
0.0
spectral coherence among center and spot position
1.0

TABLE 2. Significance analysis of paired recordings (MANOVA *P*-values) for their dependence of coherence and changes in oscillation frequency on different receptive field and stimulus properties

| | Difference in preferred orientations | Stimulus orientation | Cortical distance | Coaxiality |
|---|---|---|---|---|
| LFP low *f*: frequency | 0.214 | 0.470 | 0.011 | 0.006** |
| LFP high *f*: frequency | 0.675 | 0.000*** | 0.135 | 0.933 |
| MUA low *f*: frequency | 0.941 | 0.297 | 0.018 | 0.003** |
| MUA high *f*: frequency | 0.218 | 0.000*** | 0.993 | 0.687 |
| LFP low *f*: coherence | 0.064 | 0.732 | 0.000*** | 0.000*** |
| LFP high *f*: coherence | 0.030 | 0.478 | 0.000*** | 0.505 |
| MUA low *f*: coherence | 0.000 | 0.000*** | 0.000*** | 0.003** |
| MUA high *f*: coherence | 0.000*** | 0.000*** | 0.000*** | 0.187 |

Comparison of low-frequency ($f = 0$–$11.7$ Hz) and high-frequency ($f = 31.3$–$62.5$ Hz) signal components on the difference of preferred orientations, on stimulus orientation, on cortical distance, and on the degree of coaxiality of the orientation-sensitive neurons at pairs of recording sites. Significant dependencies are marked by asterisks (**$P < 0.01$; ***$P < 0.001$).

resembling an object's surface, while previous work reported synchronization in elongated networks resembling object contours (review in Kreiter & Singer, 1996).

Despite these major results, coherence at low and high frequencies shows similar dependencies in some aspects and different dependencies in others on stimulation, as discussed below.

### *Superiority of spectral coherence against cross-spectral power*

MUA coherence of recording pairs depends in our investigation on the relative orientation preference of the neurons, in both low- and high-frequency ranges. On a first view this seems an expected result as the spectral power at single recording positions is generally orientation specific (e.g. Koenig *et al*., 1995a; Frien *et al*., 1996; and accompanying article). Cross-spectra therefore would also reflect such orientation preferences. In particular if the recording pairs have the same preferred orientations particularly high cross-spectral values are obtained (this is due to the fact that averaging in cross-spectra is performed after calculation of the single-epoch absolute values from the complex ones). However, this introduces erroneous dependence of coupling on orientation. We therefore decided to quantify functional coupling by spectral coherence and not by cross-power spectra. The former is estimated in each frequency bin by normalization to the product of the respective power at that frequency bin and therefore eliminates orientation-tuning effects. Coherence is therefore more appropriate for spectra with dominating amplitude peaks and spectrally broadly distributed noise as in the present recordings. In addition, this type of distribution has the advantage that coherence reveals better signal-to-noise ratios. Finally, the high number of averaged windows available in our investigation for the calculation of coherence reduces the bias and increases its reliability (Glaser & Ruchkin, 1976; see Materials and methods).

### *MUA coherence is more stimulus specific than LFP coherence*

LFP coherence does not significantly change with stimulus orientation, neither at low nor at high frequencies. This is probably due to the large cortical range over which postsynaptic signals contribute to LFPs via extracellular volume conduction (spatial decay constant ~ 500 µm). This range spans the width of a typical hyper column containing neurons of every orientation preference (Hubel & Wiesel, 1968). In contrast, volume conduction of MUA plays a negligible role because of its short space constant (~ 50 µm; Gray *et al*., 1995) explaining the higher specificity of MUA compared with LFP orientation tuning (Frien *et al*., 2000).

### *Coherence of low- and high-frequency components declines with cortical distance*

The spatial decays of LFP and MUA coherence have shallower slopes than expected from volume conduction. Hence, these differences must be due to cortical connectivity. As the typical hyper column in V1 is an elongated patch of ~ 1 $mm^2$, coherence is strongly influenced by circuits spanning several hyper columns. This is particularly true for coherence among recording pair sites with similar orientation preferences (Fig. 6). This finding is in line with intracellular recordings from cat V1 (Fregnac *et al*., 1996a,b) and optical recordings from monkey V1 (Grinvald *et al*., 1994) showing subthreshold receptive fields and cortical point spread functions extending over similar ranges as does coherence in our extracellular recordings. However, in cases where single-cell spike recordings are taken for analyses of distance-depending coupling in other cortical areas, interactions were found to be restricted to much narrower ranges showing significant coupling mainly within a single column and recordings from the same electrode (parietal areas: Lee *et al*., 1998; infero-temporal areas: Gochin *et al*., 1991). This result is not conflicting with our results of broader interactions, because also in V1, single cells are weakly coupled so that long-range interactions seldom arrive at levels above that defined by the independent stochastic components of single-cell spike trains.

Although some of our recording pairs are slightly deviating from this general observation of declining coherence with distance, we did not find, e.g. an LFP coherence of 0.8 at greater and equal to 2.25 mm distance, while this value is quite common at 0.75 mm separation. This seems to contradict previous results on long-range coupling at high frequency where one case was reported with a single unit pair coupled over a distance of more than 7 mm in cat V1 (Gray *et al*., 1989). However, this remained the only report on such long-distance coupling in visual cortical structures even though many broadly spaced recordings have been made since then (Eckhorn, 1999). As we investigated average coupling values derived from local populations, rare long-range interactions would average out in our sample.

Our results also seem to contradict those of Koenig *et al*. (1995b); they reported coupling across far cortical distances in V1 of anaesthetized cats to be dominated by synchronized fast oscillations, which led them to suggest that synchronization of fast oscillations supports long-distance feature binding. These authors defined 'long distance' as > 1.5 mm. However, with our large sample of recordings in this range ($n = 217$ for $d > 1.5$ mm; see Table 1), coherence declines in any case with distance. In particular, low-frequency coherence declines more slowly than coherence of fast oscillations, which

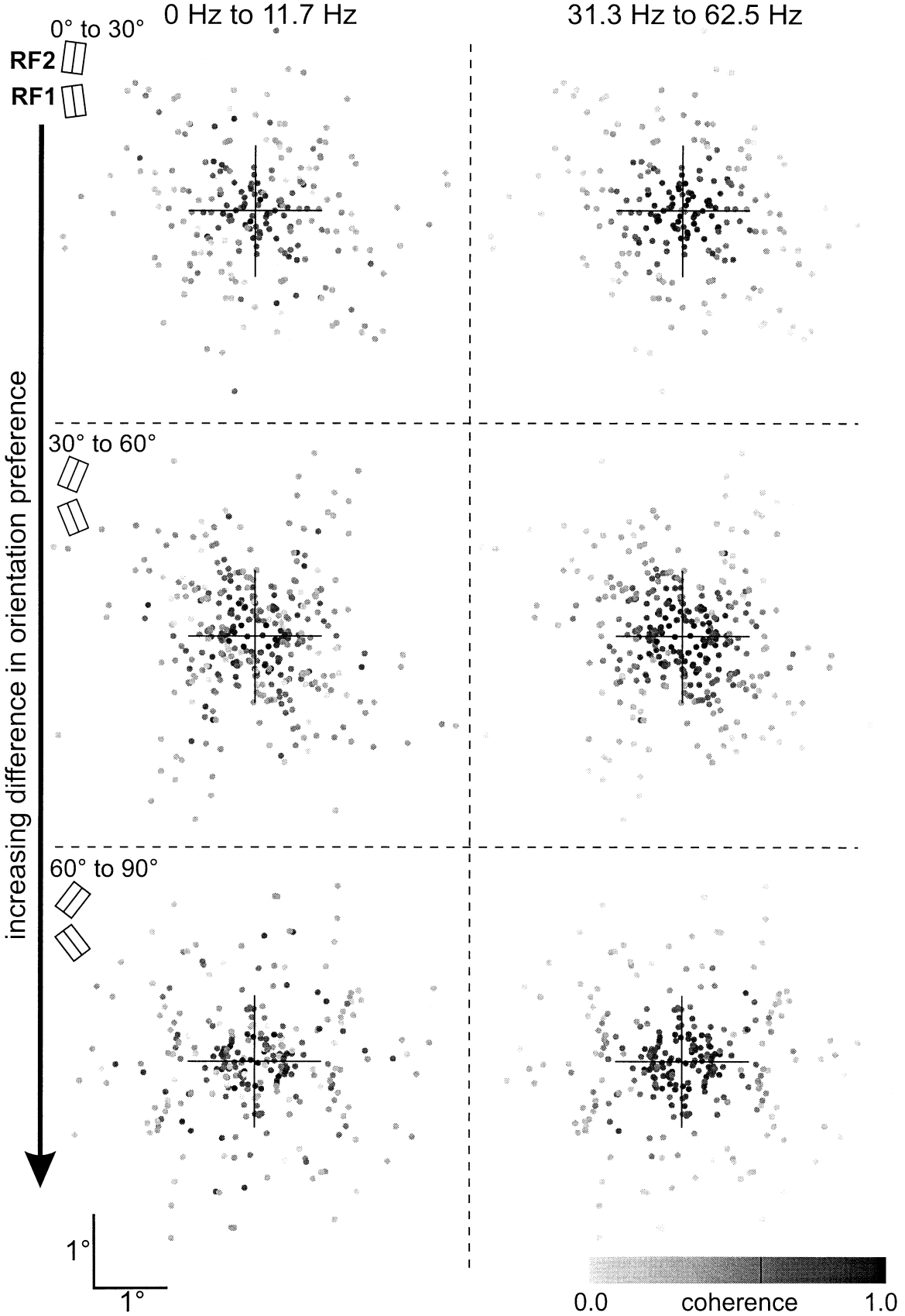


FIG. 5. 'Association field' determined from local field potentials (LFP). Distribution of cortical coupling strength among pair recording positions projected to the visual field. Coupling strengths quantified by the spectral coherence in two frequency bands (0–11.7 Hz and 31.3–62.5 Hz). More details of analysis in the caption of Fig. 4.

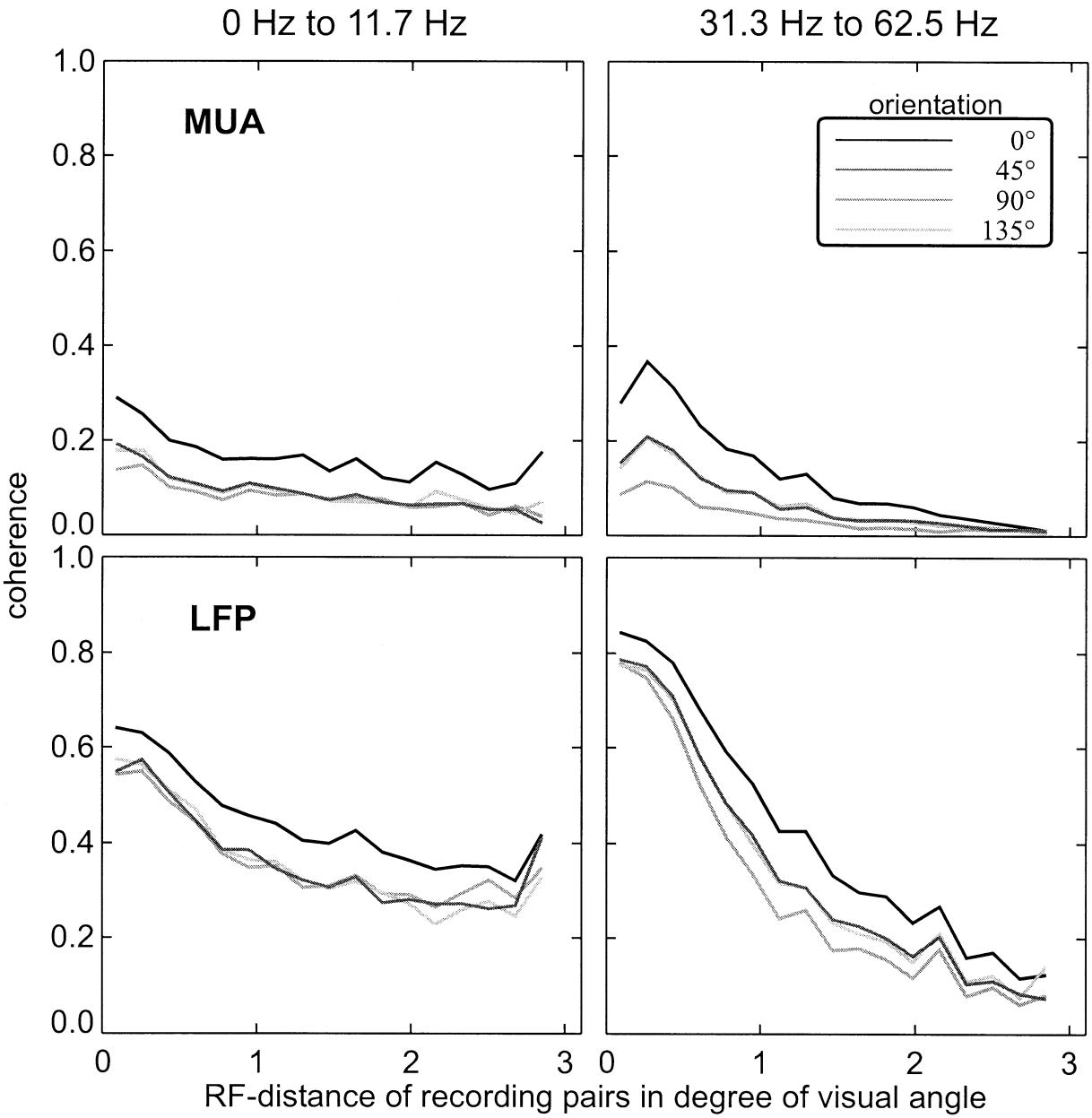


FIG. 6. Dependence of average coupling strength on distance in receptive field separation among pairs of cortical recording sites. Reference position of one RF-centre is at zero distance. Coupling strength is quantified as spectral coherence [Eq. (1)] of the dominant components in the low (0–11.7 Hz) and high (31.3–62.5 Hz) frequency bands among pairs of cortical recording sites. The different curves indicate average values of coherence derived from the smooth coherence tuning curves (see Fig. 1). Insert: 0° orientation is the normalized orientation where the coherence is maximal (see Fig. 1). 45°, 90° and 135° indicate orientation angles relative to this maximum. MUA, multiple unit activity; LFP, local field potential, both extracted from the same broad band recording.

supports earlier reports on this topic (Juergens *et al*., 1996). Our present investigation cannot solve the differences to the cited work, they may be due to the different stimuli (contour versus texture surface) and the state of the animals (anaesthetized versus awake).

### *Reduced near-field MUA coherence*

An interesting result on distance dependence of fast oscillations is the reduced MUA coherence value for receptive field separations of less than ~0.2° visual angle (corresponding to ~0.5 mm cortical distance at ~4° foveal eccentricity and half overlap of the receptive fields; Fig. 6). This is in partial agreement with investigations in the striate cortex of anaesthetized cats (Koenig *et al*., 1995a) reporting a domination of non-oscillatory slower components for short-distance coupling (overlapping receptive fields) and domination of fast oscillations for long-distance coupling (separated receptive fields). In contrast to our present study on awake monkeys, they classified neurons with cortical distances up to 2 mm as having overlapping receptive fields. Despite this quantitative difference, the reported relation between fast and slow components is similar to the present results. We find short-distance coupling is equally influenced by fast and slow components, whereas long-range coupling is dominated by fast oscillations. In contradiction to the results of Koenig and co-workers, we find reversed conditions for distances of more than 1.5° visual angle (~3.6 mm cortex) which means that fast MUA oscillations dominate coupling only in the range from 0.2 to 1.5° visual angle. Unfortunately Koenig and co-workers did not mention how their 21 long-distance recording pairs were

distributed according to cortical distance. We therefore can not compare the distance effect found in our investigation with their data.

### *MUA coherence increases with similarity in preferred orientations*

Presumably this result just reflects the anatomical numbers and the synaptic strengths of the functional connectivity in the striate cortex found in previous work. They are larger for neurons with similar receptive field properties compared with neurons with different RF properties (Ts'o *et al*., 1986; Kisvárday & Eysel, 1992; Kisvárday *et al*., 1997; Schmidt *et al*., 1997a,b). This interpretation is further supported by the indistinguishable dependence of the coherence on orientation difference in fast and slow components. In contrast, LFP coherence is independent of locally preferred orientations. This is in good agreement with the LFP orientation tunings showing only weak preference for the optimal orientation (see the accompanying paper by Frien *et al*., 2000) which can be explained by volume conduction (see above).

### *Origin of coherence in the striate cortex*

In the present investigation we are mainly interested in the question whether stimulus-related signal coherence is a potential code for binding of local visual features. Because of the experimental techniques used here it is beyond our scope to uncover the neural mechanisms producing the measured coherence. In principle, coherence in all frequency ranges can be introduced by inputs that are common to the recording positions. Common input in the striate cortex can be afferent input from thalamic or cortical sources. Coherence can also emerge with symmetric lateral connections whose activation delays are short relative to the period of the coherent frequency (Gerstner *et al*., 1993; Saam *et al*., 1999). Often fast cortical interactions, including synchronized gamma-oscillations, are interpreted as a result of lateral cortical connections without sufficient experimental proof. This is problematic as demonstrated by a recent report (Brody, 1998). He showed that slow covariations in neuronal resting potentials can lead to sharp correlogram peaks, and hence produce high-frequency coherence if the post-stimulus time histograms (PSTHs) of these activities also show sharp peaks. Thus, coherence due to such effects is easily misinterpretable as being caused by fast intracortical interactions.

However, there are several reasons why we assume that lateral striate connections contribute substantially to the high-frequency coherence in our measurements. First, Engel *et al*., (1991a) made pair recordings of fast oscillations in V1 of anaesthetized cats that were disrupted in their coherence but continued oscillating when the lateral connections in V1 were cut. Second, Gail *et al*. (1999) measured coherent fast oscillations in V1 of awake monkeys that were induced by a large grating texture. Shifting a rectangular part of the grating produced an object boundary whose cortical representation intersected the two recording positions. Also in this case, oscillations in the object and background positions continued while object-to-background coherence was abolished. The easiest explanation of coherence reduction in both experiments is functional disruption of horizontal connections. Thus, it is probable for the present investigation that coherence in the high-frequency range is substantially mediated by horizontal striate connections. In addition, misinterpretations of coherence as lateral couplings in the sense of Brody (1998) are probably not present in our investigation because the response epochs taken for coherence analysis did not show sharp structures in their PSTHs.

### *Spatially homogenous coupling may support binding of surface features*

It is an unexpected result of the present investigation to find independence of high-frequency coupling on the degree of coaxiality of the receptive fields. With the large texture gratings we find homogenous circular cortical patches in which the coherence declines with distance (Figs 4 and 5). This means that the coherence at a given distance had equal values at parallel, oblique or coaxial relative positions of the receptive field pairs. In contrast, previous work on fast oscillations in the striate cortex found generally highest values of coherence among neurons with coaxially aligned receptive fields (Gray *et al*., 1989, 1992; Engel *et al*., 1990, 1991a,b; Kreiter & Singer, 1992; Koenig *et al*., 1995a; Munk *et al*., 1996; Sengpiel *et al*., 1997). In addition, psychophysical work supports these findings by demonstrating reduced thresholds and enhanced sensitivities with coaxially aligned visual stimuli (Field *et al*., 1993; Kapadia *et al*., 1995; Polat & Norcia, 1996; Polat *et al*., 1998; Ito *et al*., 1998). Our observation of significantly higher stimulus dependence of low-frequency coherence along coaxial receptive field positions (here along the grating's stripes) compared with other relative RF positions seems to support coding along contours by low-frequency coupling. Even though we did not use contour stimuli, the finding of low-frequency coherence in our experiments may not be astonishing because neurons with similar receptive fields lying along the same stripe of a grating are simultaneously modulated coherently in their rates due to stimulus drift and residual eye motion during fixation. However, the absolute value of low-frequency coherence was considerably less than coherence of fast oscillations, even in coaxial RF directions. In summary, it is not clear from previous results and our results whether low-frequency coherence can dominate continuity coding at contours. For clarification, broad band measurements of coherence are required during stimulation with object contour stimuli.

The differences between this and previous work with respect to high-frequency coherence may be explained by differences in stimulation. While we used a large texture grating resembling the surface of an object (the texture's boundary was concentric and far outside the neurons' receptive fields), previous work found coupling among aligned neurons with stimuli resembling elongated object contours. This suggests that coupling of fast oscillations can flexibly match to spatial aspects of stimulus context: the cortical network can engage in one-dimensional groups resembling object contours and it is also able to couple neurons representing object surfaces, as shown in the present investigation.

## Acknowledgements

We thank Prof. R. Bauer, A. Guettler and T. Woelbern for help in conducting the experiments, H.-J. Brinksmeyer for revisions in artwork, U. Thomas and W. Gerber for technical support, and two anonymous referees for their constructive suggestions for improving an earlier version of the manuscript. This study was supported by the German Research Council (DFG Ec53/7 and Ro529/12 given to R.E.).

## Abbreviations

LFP, local slow-wave field potential (0.1–140 Hz); MUA, multiple unit activity (reflects all spike components picked up by a single electrode); OI, orientation index; PSTH, post-stimulus time histogram; RF, receptive field; VEP, visual evoked potentials.

## References

Brody, C. (1998) Slow covariations in neuronal resting potentials can lead to artefactually fast cross-correlations in their spike trains. *J. Neurophysiol.*, **80**, 3345–3351.

Bullock, T.H. & McClune, M.C. (1989) Lateral coherence of the electro-

corticogram: a new measure of brain synchrony. *Electroencephalogr. Clin. Neurophysiol.*, **73**, 479–498.
Eckhorn, R. (1999) Neural mechanisms of scene segmentation: recordings from the visual cortex suggest basic circuits for linking field models. *IEEE Transact. Neural Networks*, **10**, 464–479.
Eckhorn, R., Bauer, R., Jordan, W., Brosch, M., Kruse, W., Munk, M. & Reitboeck, H.J. (1988) Coherent oscillations: a mechanisms of feature linking in the visual cortex? *Biol. Cybernetics*, **60**, 121–130.
Eckhorn, R., Frien, A., Bauer, R., Woelbern, T. & Kehr, H. (1993) High frequency (60–90 Hz) oscillations in primary visual cortex of awake monkey. *Neuroreport*, **4**, 243–246.
Eckhorn, R. & Gabriel, A. (1999) Phase continuity of fast oscillations may support the representation of object continuity in striate cortex of awake monkey. *Soc. Neurosci. Abstr.,* **25**, 677.
Eckhorn, R., Reitboeck, H.J., Arndt, M. & Dicke, P. (1990) Feature linking via synchronization among distributed assemblies: simulations and results of cat visual cortex. *Neural Computation*, **2**, 293–307.
Edwards, D.P., Purpura, K.P. & Kaplan, E. (1995) Contrast sensitivity and spatial frequency response of primate cortical neurons in and around the cytochrome oxidase blobs. *Vision Res.*, **35**, 1501–1523.
Engel, A.K., Koenig, P., Gray, C.M. & Singer, W. (1990) Stimulus-dependent neuronal oscillations in cat visual cortex: inter-columnar interactions as determined by cross-correlation analysis. *Eur. J. Neurosci.*, **2**, 588–606.
Engel, A.K., Koenig, P., Kreiter, A.K. & Singer, W. (1991a) Interhemispheric synchronization of oscillatory neuronal responses in cat visual cortex. *Science*, **252**, 1177–1179.
Engel, A.K., Koenig, P. & Singer, W. (1991b) Direct physiological evidence for scene segmentation by temporal coding. *Proc. Natl Acad. Sci. USA*, **88**, 9136–9140.
Field, D.J., Hayes, A. & Hess, R.F. (1993) Contour integration by the human visual system: evidence for a local association field. *Vision Res.*, **33**, 173–193.
Fregnac, Y., Bringuier, V. & Chavane, F. (1996b) Synaptic integration fields and associative plasticity of visual cortical cells in vivo. *J. Physiol.* (*Paris*), **90**, 367–372.
Fregnac, Y., Bringuier, V., Chavane, F., Glaeser, L. & Lorenceau, J. (1996a) An intracellular study of space and time representation in primary visual cortical receptive fields. *J. Physiol.* (*Paris*), **90**, 189–197.
Frien, A., Eckhorn, R., Bauer, R. & Woelbern, T. (2000) Fast oscillations display sharper orientation tuning than other response measures in striate cortex of awake monkey. *Eur. J. Neurosci.*, **12**, 1453–1465.
Frien, A., Eckhorn, R. & Reitboeck, H.J. (1996) Fast oscillations in V1 of awake monkey: synchronization depends on cortical distance, on angle between preferred orientations and on stimulus orientation. *Soc. Neurosci. Abstr.*, **22**, 644.
Gail, A., Brinksmeyer, H.J., Eckhorn, R. & Thomas, U. (1999) Contributions of spike-rate and precise correlations to visual object representation in striate cortex of awake monkey. *Soc. Neurosci. Abstr.*, **25**, 270.5.
Gawne, T.J., Kjaer, T.W. & Richmond, B.J. (1996) Latency: another potential code for feature binding in striate cortex. *J. Neurophysiol.*, **76**, 1356–1360.
Gerstner, W., Ritz, R. & van Hemmen, J.L. (1993) A biologically motivated and analytically soluble model of collective oscillations in the cortex. I. Theory of weak locking. *Biol. Cybernetics*, **68**, 363–374.
Gilbert, C.D., Das, A., Ito, M., Kapadia, M. & Westheimer, G. (1996) Spatial integration and cortical dynamics. *Proc. Natl Acad. Sci. USA*, **93**, 615.
Glaser, E.M. & Ruchkin, D.S. (1976) *Principles of Neurobiological Signal Analysis*, 1st edn. Academic Press, New York.
Gochin, P.M., Miller, E.K., Gross, C.G. & Gerstein, G.L. (1991) Functional interactions among neurons in temporal cortex of the awake macaque. *Exp. Brain Res*., **84**, 505–516.
Gray, C.M., Engel, A.K., Koenig, P. & Singer, W. (1992) Synchronization of oscillatory neuronal responses in cat striate cortex: temporal properties. *Vis. Neurosci.*, **8**, 337–347.
Gray, C.M., Koenig, P., Engel, A.K. & Singer, W. (1989) Oscillatory responses in cat visual cortex exhibit inter-columnar synchronization which reflects global stimulus properties. *Nature*, **338**, 334–337.
Gray, C.M., Maldonado, P.E., Wilson, M. & McNaughton, B. (1995) Tetrodes markedly improve the reliability and yield of multiple single-unit isolation from multi-unit recordings in cat striate cortex. *J. Neurosci. Meth.*, **63**, 43–54.
Grinvald, A., Lieke, E.E., Frostig, R.D. & Hildesheim, R. (1994) Cortical point-spread function and long-range lateral interactions revealed by real-time optical imaging of macaque monkey primary visual cortex. *J. Neurosci.* , **14**, 2545–2568.
Hubel, D.H. & Wiesel, T.N. (1968) Receptive fields and functional architecture of monkey striate cortex. *J. Physiol. (Lond.)*, **195**, 215–243.
Ito, M., Westheimer, G. & Gilbert, C.D. (1998) Attention and perceptual learning modulate contextual influences on visual perception. *Neuron*, **20**, 1191–1197.
Juergens, E., Eckhorn, R., Frien, A. & Woelbern, T. (1996) Restricted coupling range of fast oscillations in striate cortex of awake monkey. In Elsner, N. & Schnitzler, H.-U. (eds), *Göttingen Neurobiology Report.* Thieme, Stuttgart, p. 418.
Kapadia, M.K., Ito, M., Gilbert, C.D. & Westheimer, G. (1995) Improvement in visual sensitivity by changes in local context: parallel studies in human observers and in V1 of alert monkeys. *Neuron*, **15**, 843–856.
Keeble, D.R.T. & Hess, R.F. (1998) Orientation masks 3-Gabor alignment performance. *Vision Res.*, **38**, 827–840.
Kisvárday, Z.F. & Eysel, U.T. (1992) Cellular organization of reciprocal patchy networks in layer III of cat visual cortex (area 17). *Neuroscience*, **46**, 275–286.
Kisvárday, Z.F., Tóth, É., Rausch, M. & Eysel, U.T. (1997) Orientation-specific relationship between populations of excitatory and inhibitory lateral connections in the visual cortex of the cat. *Cerebr. Cortex*, **7**, 605–618.
Koenig, P., Engel, A.K., Roelfsema, P.R. & Singer, W. (1995b) How precise is neural synchronization? *Neural Comput.*, **7**, 469–485.
Koenig, P., Engel, A.K. & Singer, W. (1995a) Relation between oscillatory activity and long-range synchronization in cat visual cortex. *Proc. Natl Acad. Sci. USA*, **92**, 290–294.
Kramer, A.F. & Jacobson, A. (1991) Perceptual organization and focused attention: the role of objects and proximity in visual processing. *Percept. Psychophys.*, **50**, 267–284.
Kreiter, A.K. & Singer, W. (1992) Oscillatory neuronal responses in the visual cortex of the awake macaque monkey. *Eur. J. Neurosci.*, **4**, 369–375.
Kreiter, A.K. & Singer, W. (1996) On the role of neural synchrony in the primate visual cortex. In Aertsen, A. & Braitenberg, V. (eds) *Brain Theory – Biological Basis and Computational Principles*. Elsevier, North Holland, pp. 201–227.
Lamme, V.A.F. (1995) The neurophysiology of figure-ground segregation in primary visual cortex. *J. Neurosci.* , **15**, 1605–1615.
Lamme, V.A.F., Rodriguez-Rodriguez, V. & Spekreijse, H. (1999) Separate processing dynamics for texture elements, boundaries and surfaces in primary visual cortex of the macaque monkey. *Cerebr. Cortex*, **9**, 406–413.
Lee, D., Port, N.L., Kruse, W. & Georgopoulos, A.P. (1998) Variability and correlated noise in the discharge of neurons in motor and parietal areas of the primate cortex. *J. Neurosci.* , **18**, 1161–1170.
Munk, M.H.J., Roelfsema, P.R., Koenig, P., Engel, A.K. & Singer, W. (1996) Role of reticular activation in the modulation of intracortical synchronization. *Science*, **272**, 271–274.
Opara, R. & Woergoetter, F. (1996) Using visual latencies to improve image segmentation. *Neural Comput.*, **8**, 1493–1520.
Orban, G.A. (1984) *Neuronal Operations in the Visual Cortex,* Chapter 6. Springer, Berlin, pp. 135–148.
Polat, U., Mizobe, K., Pettet, M.W. & Norcia, A.M. (1998) Collinear stimuli regulate visual responses depending on cell's contrast threshold. *Nature*, **391**, 580–584.
Polat, U. & Norcia, A.M. (1996) Neurophysiological evidence for contrast dependent long-range facilitation and suppression in the human visual cortex. *Vision Res.*, **36**, 2099–2109.
Saam, M., Eckhorn, R. & Schanze, T. (1999) Spatial range of synchronization in visual cortex is determined by lateral conduction velocity and determines RF-size at next processing level. *Soc. Neurosci. Abstr.,* **25**, 678.
Schmidt, K.E., Dae-Shik, K., Singer, W., Bonhoeffer, T. & Loewel, S. (1997a) Functional specificity of long-range intrinsic and interhemispheric connections in the visual cortex of strabismic cats. *J. Neurosci.* , **17**, 5480–5492.
Schmidt, K.E., Goebel, R., Loewel, S. & Singer, W. (1997b) The perceptual grouping criterion of colinearity is reflected by anisotropies of connections in the primary visual cortex. *Eur. J. Neurosci.*, **9**, 1083–1089.
Sclar, G., Maunsell, J.H.R. & Lennie, P. (1990) Coding of image contrast in central visual pathways of the macaque monkey. *Vision Res.*, **30**, 1–10.
Sengpiel, F., Sen, A. & Blakemore, C. (1997) Characteristics of surround inhibition in cat area 17. *Exp. Brain Res.*, **116**, 216–228.
Ts'o, D.Y., Gilbert, C.D. & Wiesel, T.N. (1986) Relationships between horizontal interactions and functional architecture in cat striate cortex as revealed by cross-correlation analysis. *J. Neurosci.* , **6**, 1160–1170.
Wertheimer, M. (1923) Untersuchungen zur Lehre von der Gestalt: II. *Psychol. Forsch*, **4**, 301–350.
Zipser, K. & Lamme, V.A.F. (1996) Contextual modulation in primary visual cortex. *J. Neurosci.*, **16**, 7376–7389.